# Synthesis of polyaniline nanofiber and anticorrosion property of polyaniline–epoxy composite coating for Q235 steel

**Cheng Yue Ge, Xiao Gang Yang, Bao Rong Hou**

**Abstract** Polyaniline (PANI) nanofibers were prepared by direct mixed oxidation in four kinds of inorganic acids. The characterization of scanning electron microscopy (SEM) showed that high quality PANI fibers with uniform diameter and several microns length can be obtained by direct mixed oxidation, especially in a sulfuric acid system. Structural characteristics of PANI products through IR and UV spectra indicated the consistent peak distribution with the classic spectrum of the doped PANI. In addition, composite coatings of PANI–epoxy resin were prepared by mechanical grinding. The effect of PANI's content on anticorrosion property of the composite coatings for Q235 steel was studied by the electrochemical impedance spectroscopy (EIS). Results showed that the best shielding protective effect was obtained when the amount of PANI was around 0.5% (wt%). More importantly, the effects of four different inorganic acids on anticorrosion property of the composite coatings were studied by the EIS and Tafel polarization curve. Experiments showed that the different composite coatings of PANI doped by different inorganic acids provided different protective abilities for the Q235 steel. It can be concluded that both the morphology and counteranion would impact the anticorrosion effect of the doped PANI.

C. Y. Ge, X. G. Yang, B. R. Hou (✉)
Institute of Oceanology, Chinese Academy of Sciences, No. 7 Nanhai Road, Qingdao 266071, China
e-mail: houbaorong@yahoo.com

C. Y. Ge
Graduate School of the Chinese Academy of Sciences, No. 19 Yuquan Road, Beijing 100049, China
e-mail: gechengyue@sina.com

## Introduction

Polyaniline (PANI) is one of the most intensively investigated conducting polymers due to its excellent environmental stability, ease of synthesis, and relatively high level of electrical conductivity.[1–4] Now, PANI has been widely studied for potential applications in many domains such as electrochromic devices, rechargeable batteries, electromagnetic interference shielding, and sensors.[5,6] Since the time Deberry[7] found the protective effect of PANI on iron-based metal, the anticorrosion application of PANI has attracted enormous interest among researchers.[8,9] However, this has been controversially discussed among the experts so far. Some studies by experts such as by Williams and McMurray[10] suggested that conducting polymers could not be used successfully for corrosion protection application, which reported enhanced corrosion by PANI, and some other studies such as by Michalic and coworkers[11,12] critically discussed the corrosion protective ability of conducting polymers. Furthermore, the benefits of PANI's application are restricted by its poor solubility, as well as infusible and almost nonprocessable properties.[13] In order to improve the application property of PANI, a number of methods, such as mixing of PANI with epoxy resin by mechanical dispersion to prepare composite coatings[14–18]; synthesis of PANI–Na–MMT clay nanocomposites to modify the application property[19]; copolymerization with water-soluble polymer through in situ polymerization to improve the water solubility[20]; and deposition on the surface of substrate metal by electrochemical techniques to protect material from corrosion were studied.[7,21,22] Among these techniques, mixing of the PANI with epoxy resin by

mechanical dispersion to prepare composite coatings is one of the most frequently used methods.

Studies on the development and application of nanotechnology in preparing PANI explored a wider range of application prospects for PANI. Nanostructure PANI carries many specific physical and chemical properties, such as specific light absorption, catalytic and magnetic properties due to the surface, quantum and macroscopic quantum tunneling influences.[23–25] Currently, the main methods of preparing PANI nanostructure are the "template" method,[26] electrochemical polymerization,[27] interfacial polymerization,[28] direct mixed reaction,[29] self-assembly method,[30] solid-state reaction method,[31] and so on. Through these methods, various nano-morphologies such as nanoparticle, nanorod, nanofiber, nanobelt, nanotube, and so on were synthesized. However, among numerous nanostructures, the nanofibers which frequently showed one-dimensional nanoscale structure were considered extensively because of their simple method of synthesis. Furthermore, it was easy to control or adjust the morphology of PANI nanofibers.[29,32]

In this article, PANI nanofibers were prepared in four kinds of common inorganic acids by direct mixed oxidation method at room temperature. Morphology of PANI was investigated by the field emission-scanning electron microscopy (FE-SEM). More importantly, effects of different inorganic acids on morphology of PANI nanofibers were studied. Further, composite coatings of epoxy resin mixed with PANI nanofibers were prepared by mechanical grinding, and then effects of PANI on anticorrosion property of composite coatings for Q235 steel were studied in detail through electrochemical impedance spectroscopy (EIS) and Tafel polarization curve.

# Experimental

## Materials

Aniline (AN), ammonium peroxydisulfate (APS), hydrochloric acid (HCl), phosphoric acid ($H_3PO_4$), nitric acid ($HNO_3$), and sulfuric acid ($H_2SO_4$) were purchased from the Industry of Fine Chemicals, Laiyang, China. Epoxy resin (828) was purchased from the Norsun Chemicals Limited Company, Langfang, China. Polyamide curing agent (450) was purchased from the Huntsman International LLC, Guangzhou, China. All the raw materials were used directly as received without purification.

## Preparation of PANI

To an aqueous solution of aniline (2 mmol) in 1 M acid (10 mL) another solution of APS (1 mmol) in 1 M acid (10 mL) was added, and this solution mixture was immediately subjected to magnetic stirring to ensure sufficient mixing before reaction. The reaction was carried out for 24 h at 25°C. The resulting PANI precipitates were purified by centrifugation using de-ionized water and ethanol until the suspension reached a neutral pH value.

## Preparation of PANI–epoxy resin composite coating

The epoxy resin used for preparing the composite coatings is a colorless, transparent liquid and possesses some physical properties, such as the epoxy equivalent weight of 184–194 g/Eq, the viscosity (at 25°C) of 11–15 Pa·s, the residual solvent weight of ≤ 500 mg/kg, and so on. The matching curing agent is yellow or brown clear liquid and possesses some physical properties, such as the amine value of 250–290 mg KOH/g, the viscosity (at 25°C) of 1–2 Pa·s, the equivalent weight of active [H] of 115 g/Eq, and so on.

A certain amount of PANI was dispersed in epoxy resin through mechanical grinding using cone-mill. Then, the mixture of epoxy and PANI was further mixed with matching curing agent in the ratio of 100:60 to obtain composite coatings.

## Characteristics

Morphology of PANI was characterized by the field-emission scanning electron microscopy (FE-SEM, JSM 6700F). Molecular structures of PANI were characterized using the VERTEX70 infrared spectrometer (using pellets with KBr) and Cary 500 UV–Vis–NIR spectrophotometer. (The products were dispersed in ethanol.)

The working electrode sample of Q235 steel of 1-cm diameter was polished progressively using 600 $\sim$ 1200-mesh abrasive paper, then cleaned, degreased and dried. It was finally coated by the composite coatings to obtain the film with a thickness of $100 \pm 10$ μm.[33] Taking platinum electrode as auxiliary electrode and saturated calomel electrode as reference electrode, the EIS and the Tafel polarization curves were analyzed using three-electrode system through PARSTAT2273 in 3.5% sodium chloride solution: with testing frequency ranging from 100 kHz to 10 mHz, disturbance amplitude of potential, 50 mV, and testing area, 0.7854 cm$^2$.

# Results and discussion

## Structure characteristic of PANI

Serving as important and basic information, the molecular structure of PANI was revealed by the IR spectrometer (Fig. 1a). It can be seen from Fig. 1a that
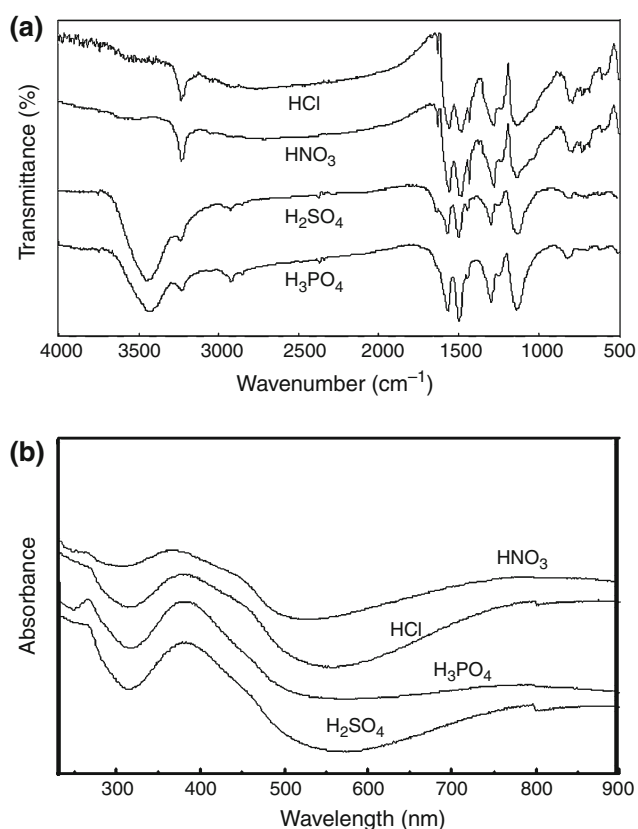
**Fig. 1: FTIR spectrum (a) and UV–Vis spectrum (b) of polyaniline doped by different acids**

the IR peak distributions of PANI products prepared in four kinds of inorganic acid are similar. In IR spectrometer, the following absorption peaks were observed: at 3300 cm$^{-1}$ corresponding to the stretching vibration absorption of N–H; at 1570 and 1480 cm$^{-1}$ corresponding to the stretching vibration absorption peaks of C=C which belong to the quinone- and benzene rings, respectively; at around 1300 cm$^{-1}$ corresponding to the stretching vibration of C–N in the benzene ring; at around 1140 and 810 cm$^{-1}$ corresponding to the plane bending vibrations of C–H which belong to quinone- and benzene rings, respectively. In addition, a weak absorption peak emerged at around 1440 cm$^{-1}$ corresponding to the plane bending vibration of the saturated C–H which indicated the presence of a conjugate structure.

As another basic structure characteristic for a product with benzene ring, the UV–Vis absorption spectra of PANI prepared in four kinds of inorganic acids are shown in Fig. 1b. It can be seen from Fig. 1b that absorption peaks have emerged at both 280 nm and 390 nm for the four samples, apart from a tailing peak that has emerged at 800 nm. Here, the absorption peak at 280 nm is attributed to $\pi$–$\pi^*$ transition of benzene ring; at 390 nm to the transition absorption of polaron to $\pi^*$, and the tail peak at 800 nm corresponds to the absorption of polaron after being doped by

proton. These data taken together further indicated that the products obtained in four kinds of inorganic acids were all doped PANI.

## The effects of different inorganic acids on product's morphology

As can be seen from Fig. 2, PANI nanofibers can be obtained in four kinds of inorganic acids. In detail, PANI obtained in HCl system possessed a uniform diameter of 100 nm, and the surface of single nanofiber is relatively smooth. However, a few PANI nanoparticles were attached to the surface of fibers, and furthermore, the length of fiber (200–400 nm) was shorter (Fig. 2a). PANI obtained in H$_3$PO$_4$ system also showed a certain fiber morphology with diameter in the range of 100–150 nm, but there were a large number of aggregated PANI nanoparticles (Fig. 2b). PANI obtained in HNO$_3$ system possessed good morphology with diameter in the range of 80–100 nm; however, the length of fibers (500–1000 nm) was also shorter (Fig. 2c). PANI obtained in H$_2$SO$_4$ system possessed the best morphology with uniform diameter of about 60 nm and the length of fibers reached several microns. Furthermore, some of fibers mingled to form the dense network structure (Fig. 2d).

In the experiment, acid solution of aniline was transparent before mixing. It is indicated that aniline existed in the form of aniline cations in strong acid. No template existed to decide the morphology of product (nontemplate theory). With respect to nanofiber formation mechanism of facile synthesis proposed by Huang and Kaner,[29] the following theory was proposed: When aniline is dissolved in the strong acids such as HCl, H$_3$PO$_4$, HNO$_3$, and H$_2$SO$_4$, aniline cations are generated. Moreover, taking direct mixed oxidation method, all of the oxidants were added at the same time and immediately stirred. Therefore, it may be recognized that the homogeneous solution had been formed before the reaction. In the homogeneous solution, aniline cations were oxidized to aniline oligomers; these oligomers were ionized immediately in the high acidity (pH < 1). The ionized aniline oligomers polymerized with adjacent aniline cations or other aniline oligomers to form PANI with a longer molecular chain. Moreover, in a strong acid, the PANI molecular chain grew one-dimensionally, along with the central line. With the growth of the molecular chain, solubility of PANI decreased gradually, and a large number of nanofibers were precipitated in the solution. Furthermore, some of these nanofibers mingled together to form network structure relying on Van der Waals force and hydrogen bond. While the aniline cations got exhausted, the residual aniline oligomers were adsorbed on the surface of fibers to form the granular aggregate.

Based on the above theory, the following deduction is justified: In the HCl system, due to the small radius, it is easy for Cl$^-$ to access into molecules of aniline
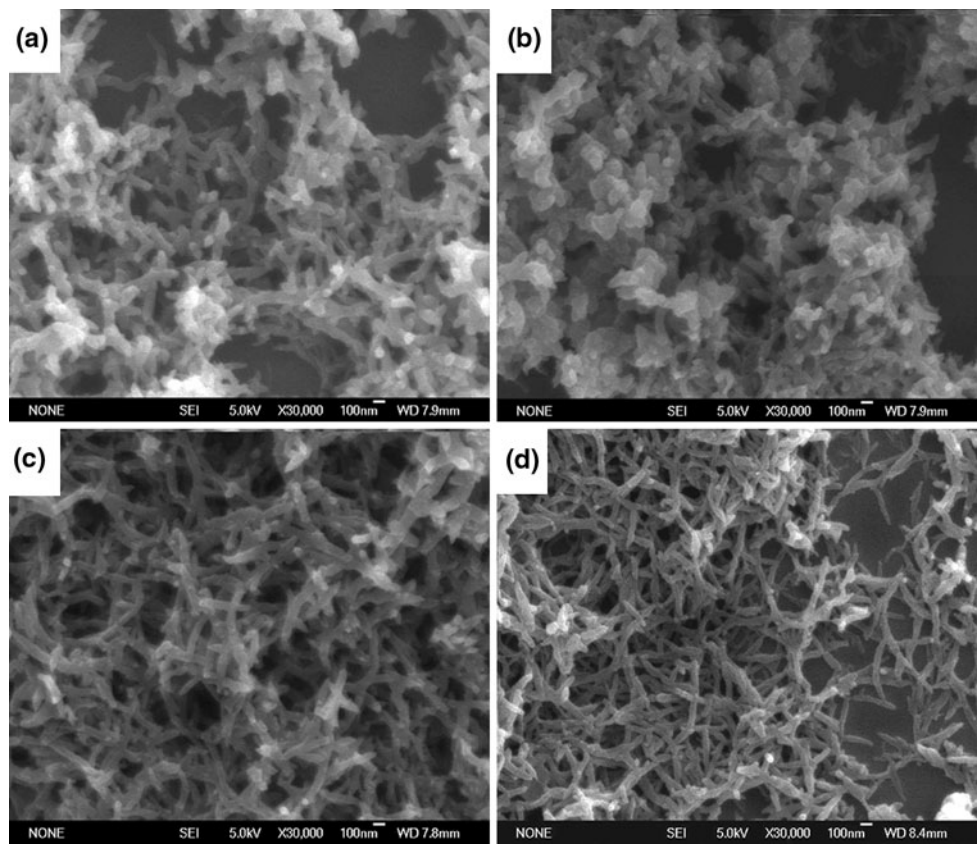
**Fig. 2: SEM images of polyaniline synthesized in different acids: (a) hydrochloric acid; (b) phosphoric acid; (c) nitric acid; (d) sulfuric acid**

oligomers to produce a greater number of ionized aniline oligomers (the active central molecules of chain growth). These ionized aniline oligomers reacted with each other to result in generation of short fibers. In the $HNO_3$ system, due to the strong oxidation of $HNO_3$, a greater number of aniline oligomers appeared in a short time. This also led to a greater number of ionized aniline oligomers and resulted in generation of shorter fibers similar to those obtained in the HCl system. In the $H_3PO_4$ system, the presence of $H_2PO_4^-$ and $HPO_4^{2-}$ had an impact on the ionization of aniline oligomer. Some nonionized aniline oligomers got attached to the fibers to form granular aggregate. In the $H_2SO_4$ system, it was beneficial for the rate of ionization (aniline oligomers) and chain growth to match because of comprehensive effects of pH, oxidation, and $SO_4^{2-}$. Therefore,

excellent fibers several microns long and with smooth surface were obtained.

## Effects of the dosage of PANI on film and anticorrosion property of epoxy resin

Selecting $H_2SO_4$-doped PANI, the composite coatings with different amount of PANI were prepared. The typical recipes are listed in Table 1. The viscosities of composite coatings without any solvent are very high (about $10^5$ mPa·s) at room temperature. Therefore, spray is needed in the practical application. However in laboratory, the testing samples were scratched on surface of plate (150 × 70 mm) or electrode using self-prepared scratcher because of restriction in the quantity. All the samples were cured at natural environment

**Table 1: Typical recipes and curing times of composite coatings with different amounts of PANI**

| Sample | 0% | 0.1% | 0.2% | 0.4% | 0.6% | 0.8% | 1% | 2% | 4% |
|---|---|---|---|---|---|---|---|---|---|
| Dosage of PANI/g | 0 | 0.04 | 0.08 | 0.16 | 0.24 | 0.32 | 0.4 | 0.8 | 1.6 |
| Dosage of epoxy resin/g | 25 | 25 | 25 | 25 | 25 | 25 | 25 | 25 | 25 |
| Dosage of curing agent/g | 15 | 15 | 15 | 15 | 15 | 15 | 15 | 15 | 15 |
| Curing times/h | ≤24 | ≤24 | ≤24 | ≤24 | ≤24 | 24–48 | 72–96 | 144–168 | >168 |
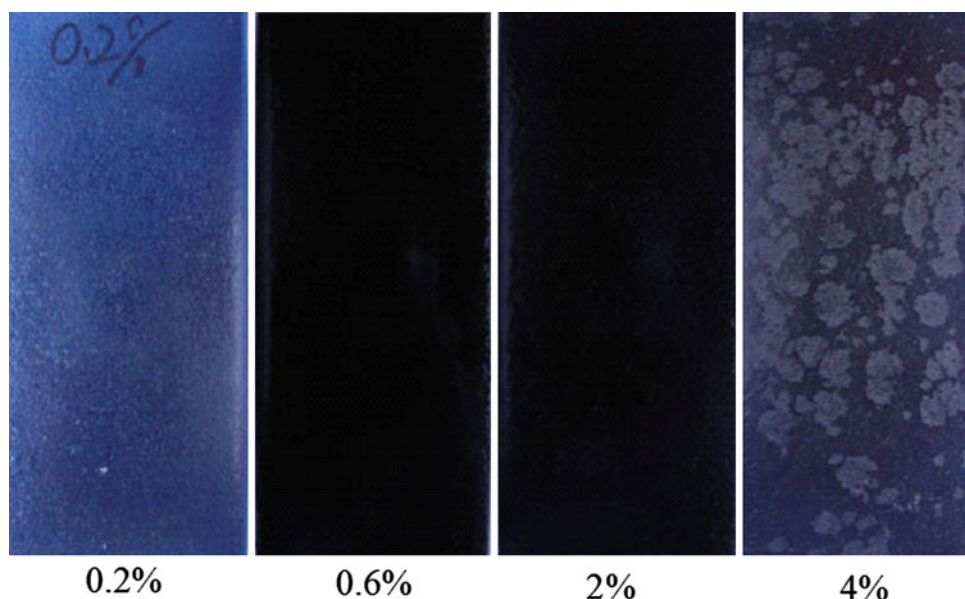
**Fig. 3: Digital photographs of composite coatings with different amounts of PANI**

(temperature: 25 ± 5°C, and relative humidity: 45 ± 5%) to obtain the films with a dry film thickness of 200 ± 20 μm or 100 ± 10 μm. The curing times are listed in Table 1. The effects of PANI's content on film-forming and anticorrosion properties of epoxy resin were investigated by digital photos and the EIS.

As can be seen from Fig. 3, the coatings looked relatively glossy, and dense coatings were obtained when the amount of PANI was less than 0.6%. In addition, the color of coating deepened gradually with the increasing dosage of PANI. As the dosage of PANI increased to 2%, visible pinhole defect emerged on the surface. When the amount of PANI reached to 4%, the defect became clear, and large areas of spots emerged on the surface. All these facts indicated that introduction of PANI impacted the film property of epoxy resin. During the experiment, it was found that composite coatings cured slowly when the dosage of PANI surpassed 1%; the higher the amount of the PANI added, the longer the curing time required. The results are listed in Table 1, but further research is needed to make the possible reason more clearly understood.

It is a simple, fast, and an effective method to study anticorrosion property of coating by the EIS plot.[34] Figures 4 and 5 are the EIS plots of composite coatings with different amounts of PANI. For the EIS curves without diffusion, equivalent circuit $R_s(R_cC)$ was chosen to fit, as shown in Fig. 6a.[34] In the figure, $R_s$ symbolizes the solution resistance, $Q_c$ symbolizes the coating capacitance, and $R_c$ symbolizes the coating resistance. For the EIS curves with evident diffusion, equivalent circuit $R_s(C(R_{po}(C_{d1}(R_tW))))$ was chosen to fit, as shown in Fig. 6b.[34] In this figure, $Q_{d1}$ symbolizes the double electric layer capacitance, $R_{po}$ symbolizes the porous resistance (the same as with the $R_c$), $R_t$ symbolizes the charge transfer resistance, and $Z_w$

symbolizes the Weber impedance. The fitting values are shown in Table 2.

It can be seen from Fig. 4 and Table 2, that at the initial immersed stage, with increasing dosage of PANI, the value of $R_c$ increased first and then decreased. The greatest value appeared when the dosage of PANI was 0.6%. In addition, when the dosage of PANI did not surpass 1%, the $R_c$ values of composite coatings were greater than the value of pure epoxy coating ($R_c$ = 1.339E9). This fact showed that the introduction of PANI improved the anticorrosion property of the composite coating. While the dosage of PANI increased to 2%, the EIS plot showed evident diffusion, which indicated that the composite coating was damaged, and corrosion was caused on the metal (Fig. 4, inset diagram).

After being immersed for 7 days, it can be seen that (Fig. 5; Table 2) the value of $R_c$ was still very high when the dosage of PANI was 0.6%, but $R_c$ value of pure epoxy coating decreased significantly ($R_{po}$ = 2.284E6). This fact further proved that PANI can improve the protective effect of the epoxy coating. Surprisingly, when the dosage of PANI was 1.0%, the $R_c$ value of composite coating decreased more drastically ($R_{po}$ = 1.456E6). This was because the poor dispersion of the higher amount of PANI in the epoxy resin impacted the compactness of the coating. It was easy for the corrosion medium to permeate into the coating and damage it.

## Anticorrosion properties of PANIs doped by different acids for Q235 steel

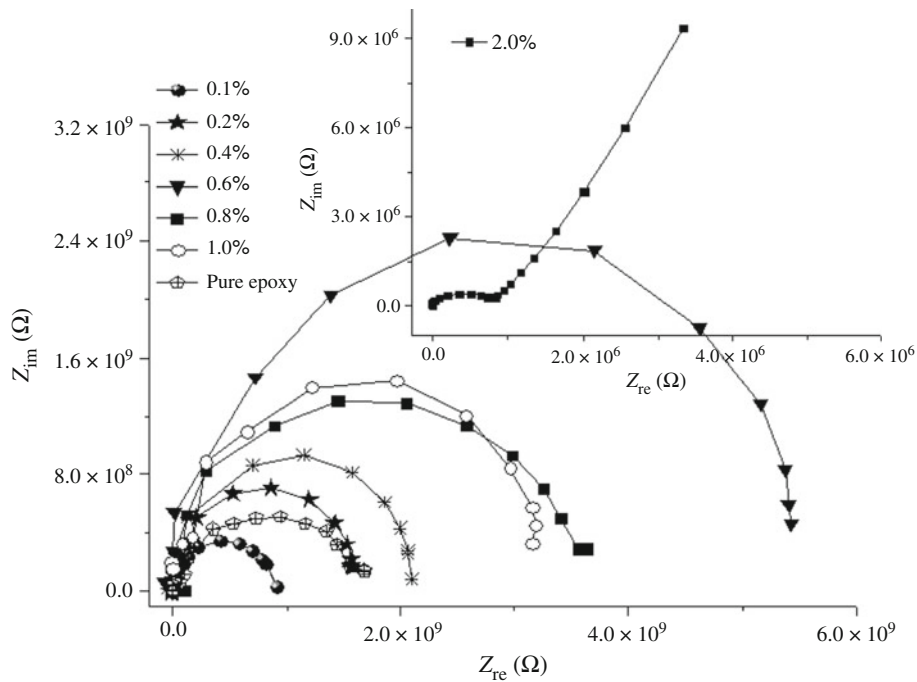Fixing the PANI's content at 0.5% (wt%), the epoxy composite coatings mixed with different PANIs doped

**Fig. 4: EIS plots of epoxy coatings mixed with different amounts of PANI before immersion**
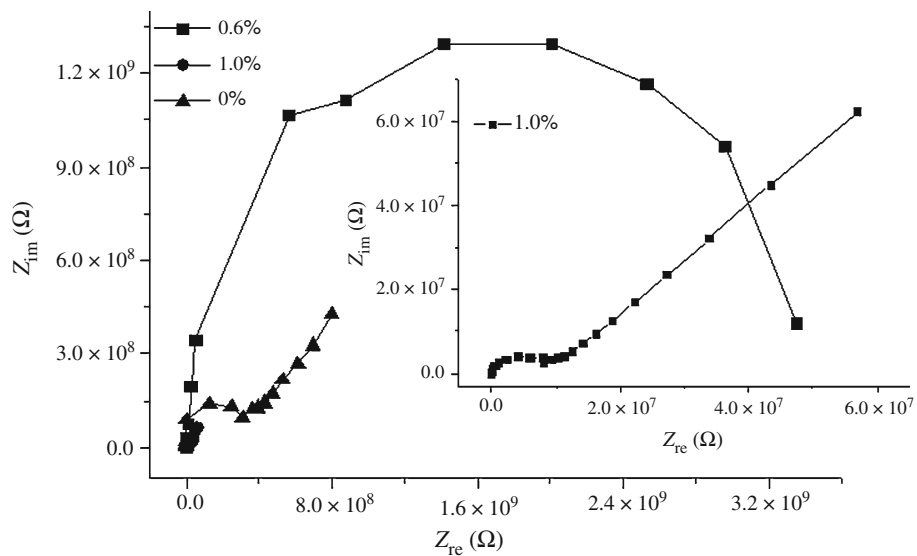


**Fig. 5: EIS plots of epoxy coatings mixed with different amounts of PANI after being immersed for 7 days**

by four different acids were obtained. The anticorrosion property at different immersion times was studied using the EIS and Tafel polarization curves as shown in Figs. 7–11. For the EIS curves without diffusion, the equivalent circuit $R_s(R_cC)$ was chosen to fit, as shown in Fig. 6a. For the EIS curves of two approximately semicircular shapes, the equivalent circuit $R_s(R_cC)$ $(R_cC)$ was chosen to fit, as shown in Fig. 6c. The fitting values are shown in Table 3.

It can be seen from Figs. 7–10 that during the immersion time, the excellent protective effect for Q235 steel was provided by the composite coatings mixed with the PANI doped by $HNO_3$, $H_2SO_4$, and $H_3PO_4$. The values of the coating resistance were still high even after immersion of the material for 168 h. For the composite coating mixed with HCl-doped PANI, corrosion occurred on the substrate after being immersed for 24 h. On further analyzing the data given
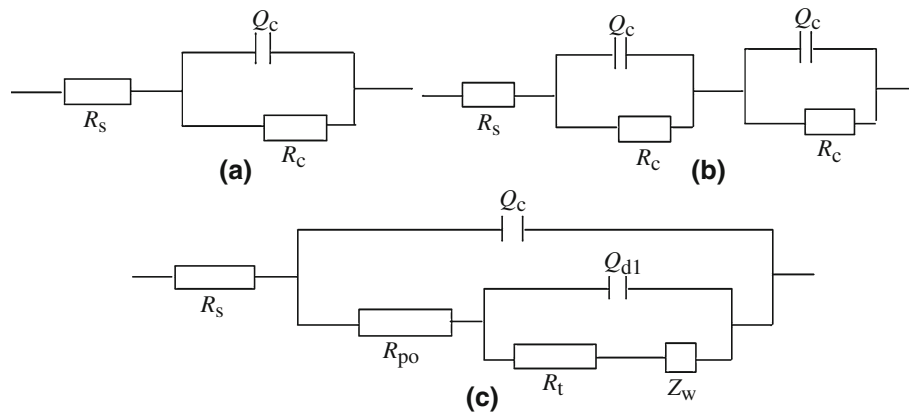
**Fig. 6: Equivalent circuits of the EIS plots: (a) without diffusion; (b) with diffusion; (c) with two semicircles**

**Table 2: Fitting values of EIS plots of epoxy coatings mixed with different amounts of PANI**

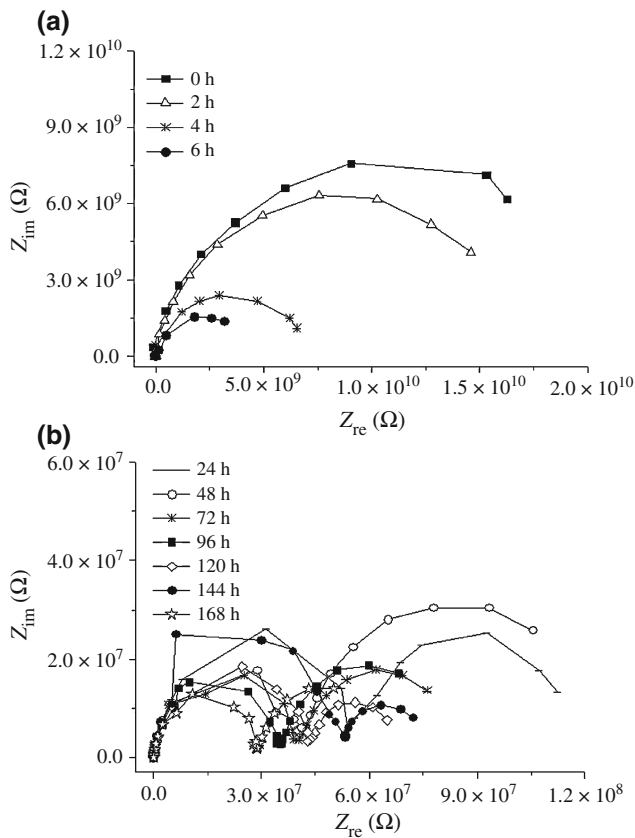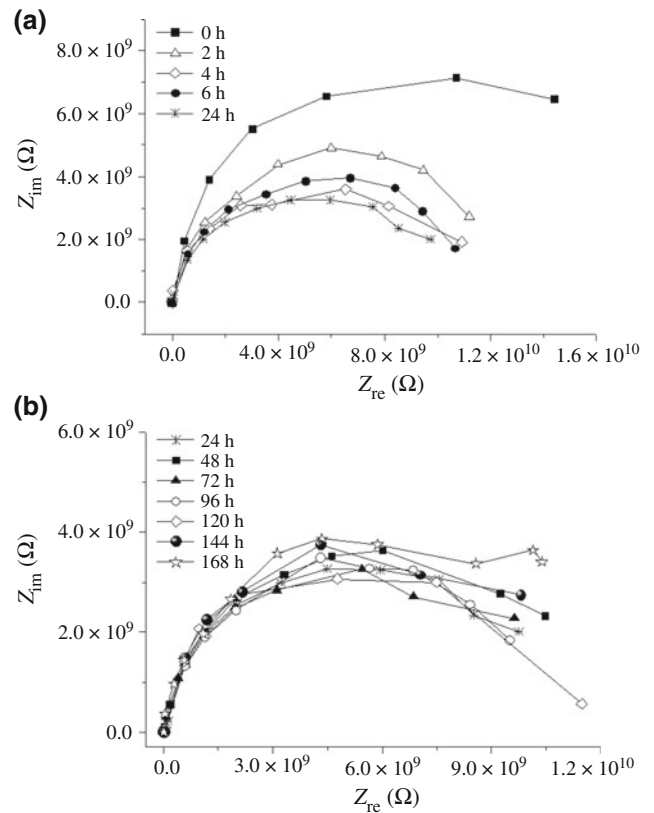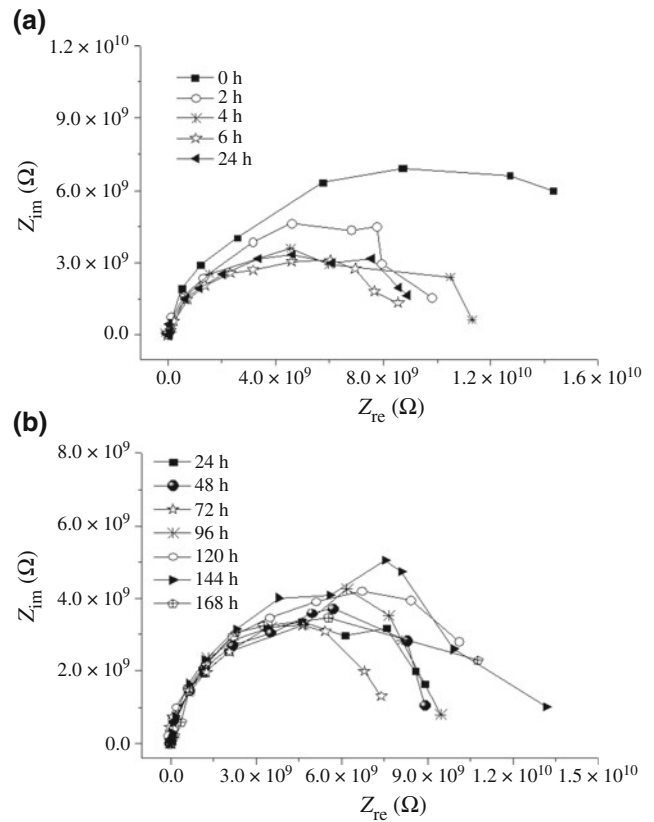| Before immersion | Content of PANI | 0 | 0.1% | 0.2% | 0.4% | 0.6% | 0.8% | 1.0% | 2.0% |
|---|---|---|---|---|---|---|---|---|---|
| | $R_c/\Omega\ cm^2$ | 1.339E9 | 8.071E8 | 1.551E9 | 2.062E9 | 5.117E9 | 3.141E9 | 3.071E9 | 2.369E6 |
| After being immersed for 7 days | Content of PANI | 0 | 0.6% | 1.0% | | | | | |
| | $R_{po}(R_c)/\Omega\ cm^2$ | 2.284E6 | 3.054E9 | 1.456E6 | | | | | |



**Fig. 7: EIS plots of epoxy coatings mixed with HCl-doped PANIs at different immersion times: (a) 0–6 h; (b) 24–168 h**

**Fig. 8: EIS plots of epoxy coatings mixed with HNO₃-doped PANI at different immersion times: (a) 0–24 h; (b) 24–168 h**

**(a)**



**(b)**
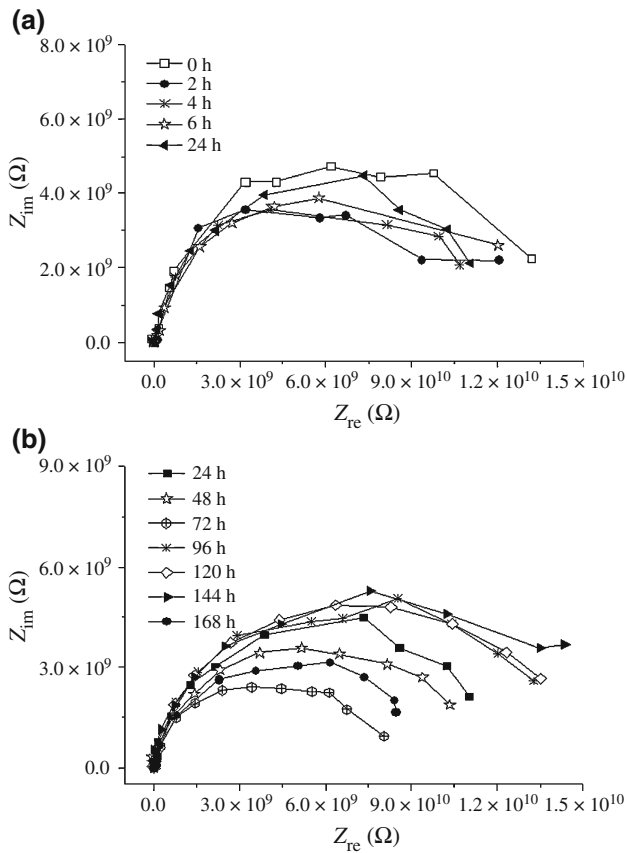


**Fig. 9: EIS plots of epoxy coatings mixed with H$_2$SO$_4$-doped PANI at different immersion times: (a) 0–24 h; (b) 24–168 h**

**(a)**



**(b)**



**Fig. 10: EIS plots of epoxy coatings mixed with H$_3$PO$_4$-doped PANI at different immersion times: (a) 0–24 h; (b) 24–168 h**

in Table 3, it was found that with the extension of soaking time, the $R_c$ value of composite coating mixed with HCl-doped PANI decreased gradually. After being immersed for 24 h, the value of $R_c$ decreased to $10^{7}$, which indicated that corrosion had occurred. Interestingly, the $R_c$ value showed recovery sign after being immersed for 3 months. The $R_c$ value of composite coating mixed with HNO$_3$-doped PANI decreased first and stabilized gradually after 24 h, the values being maintained at 8.3E9–8.9E9, which indicated good protective effect. After being immersed for 3 months, the $R_c$ was still maintained at a relatively high value (5.550E9). The $R_c$ values of composite coatings mixed with H$_2$SO$_4$- and H$_3$PO$_4$-doped PANIs decreased first and recovered gradually to their initial levels after being immersed for 72 h. After being immersed for 3 months, the $R_c$ still maintaining very high values showed the superior protective effect.

From Tafel polarization curves, it can be observed that the anticorrosion properties of different PANI-epoxy composite coatings were further revealed clearly and directly. It can be seen from Fig. 11 and Table 4 that the composite coatings mixed with H$_3$PO$_4$-doped PANI indicated the highest corrosion potential ($V_{corr} = -30.785$ mV) which was higher than the self-corrosion

potential of Q235 steel ($V_{corr} = -0.69$ to $-0.66$).[35] The corrosion potential of composite coating mixed with H$_2$SO$_4$-doped PANI, $V_{corr} = -127.108$ mV, was also higher than the self-corrosion potential of Q235 steel. Then, the corrosion potential of composite coatings mixed with HNO$_3$-doped PANI, $V_{corr} = -437.347$, was still higher than self-corrosion potential of Q235 steel. Composite coating mixed with HCl-doped PANI showed the lowest corrosion potential, $V_{corr} = -651.959$, which was close to the self-corrosion potential of Q235 steel. However, the sequence of the corrosion current ($I_{corr}$) is just the opposite. All these data showed that composite coatings mixed with H$_3$PO$_4$-doped PANI showed the best protective effect, followed by composite coating mixed with H$_2$SO$_4$-doped PANI, and then this was followed by the composite coating mixed with HNO$_3$-doped PANI. The composite coating mixed with HCl-doped PANI provided the worst protective effect.

In a metallic corrosion environment, the doped PANI (Emeraldine base) was prone to be reduced to release the counter-anion and thus become de-doped PANI (Lecucoemeradine base).[36] The Cl$^-$ released from the HCl-doped PANI was the crude corrosion medium and would promote corrosion to accelerate
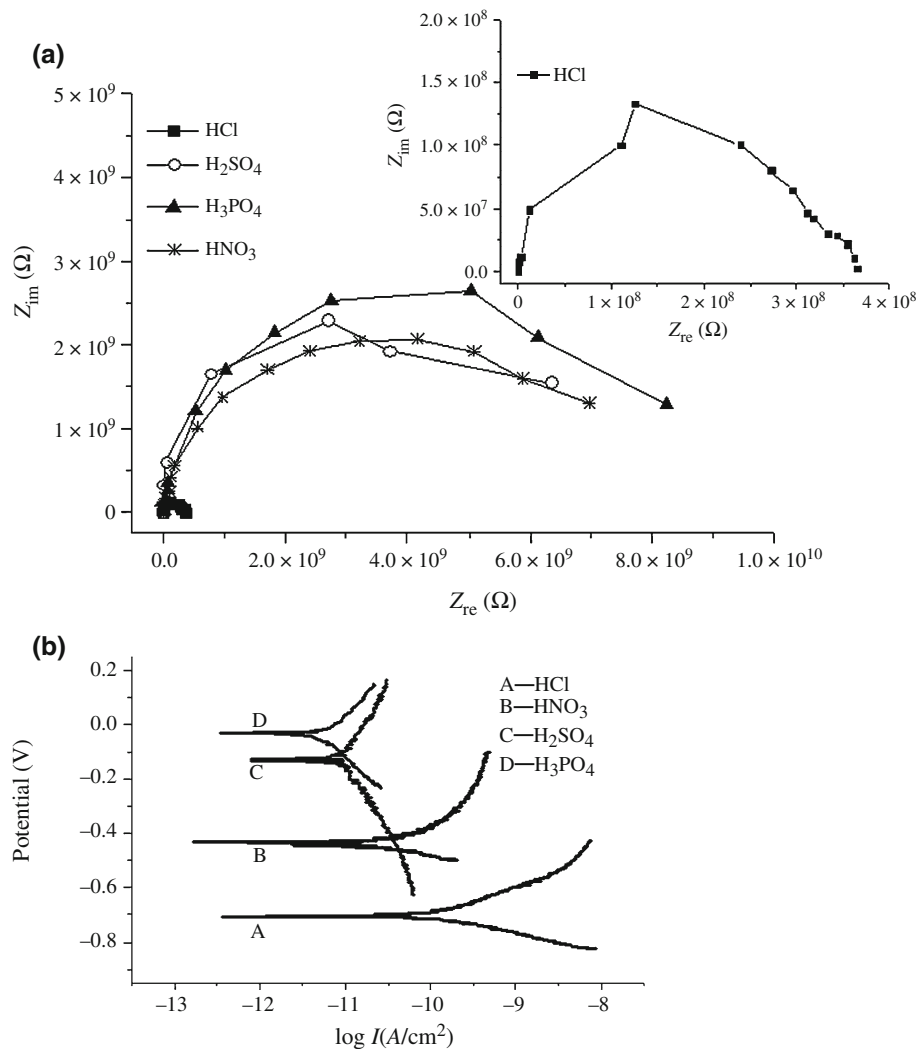
**Fig. 11: EIS plots (a) and Tafel polarization curve (b) of epoxy coating mixed with different PANIs after being immersed for 3 months**

**Table 3: Fitting values of EIS plots of different composite coatings at different immersion times**

| Immersion times | Acid kinds | | | |
|---|---|---|---|---|
| | HCl | HNO$_3$ | H$_2$SO$_4$ | H$_3$PO$_4$ |
| $R_c(R_{po})$/Ω cm$^2$ | | | | |
| 0 h | 1.633E10 | 1.786E10 | 1.125E10 | 1.482E10 |
| 2 h | 1.361E10 | 1.046E10 | 8.552E9 | 1.013E10 |
| 4 h | 5.889E9 | 9.346E9 | 9.743E9 | 9.126E9 |
| 6 h | 3.334E9 | 9.308E9 | 9.679E9 | 7.834E9 |
| 24 h | 5.499E7/5.579E7 | 8.450E9 | 9.897E9 | 7.434E9 |
| 48 h | 4.161E7/6.640E7 | 8.820E9 | 8.877E9 | 7.344E9 |
| 72 h | 3.999E7/3.988E7 | 8.993E9 | 6.443E9 | 6.947E9 |
| 96 h | 3.499E7/3.506E7 | 8.299E9 | 1.162E10 | 8.415E9 |
| 120 h | 4.222E7/4.094E7 | 8.580E9 | 1.180E10 | 9.161E9 |
| 144 h | 5.134E7/5.125E7 | 8.669E9 | 1.186E10 | 1.054E10 |
| 168 h | 2.843E7/2.867E7 | 8.422E9 | 7.786E9 | 9.777E9 |
| 3 months | 3.260E8 | 5.550E9 | 6.255E9 | 6.603E9 |

**Table 4: Fitting values of Tafel curve of different composite coatings after being immersed for 3 months**

| Acid kinds | HCl | HNO$_3$ | H$_2$SO$_4$ | H$_3$PO$_4$ |
|---|---|---|---|---|
| $E_{corr}$ (mV) | −651.959 | −437.347 | −127.108 | −30.785 |
| $I_{corr}$ (A/cm$^2$) | 1.175E−4 | 8.532E−5 | 9.090E−6 | 8.830E−6 |

the damage to coating. The increase of $R_c$ value after being immersed for 3 months may be caused by the shielding effect of Lecucoemeradine-based PANI or corrosion products.[37] The $PO_4^{3-}$ released from H$_3$PO$_4$-doped PANI possessed catalytic function to passive metal which would help form excellent passive film on the substrate surface. Moreover, $PO_4^{3-}$ can react with corrosion products to produce dense complex film to provide protection.[8,38] In the case of the composite coatings mixed with H$_2$SO$_4$, and HNO$_3$-doped PANIs, the superior protection should be attributed to their excellent fiber morphology and network structure. The doped PANI was provided with relatively high level of conductivity and interesting redox property. As for the doped PANI with long fibers and network structure, it was easier to form a conductive pathway in the coating and take place of redox reaction with substrate to passive metal or separate cathode and anode reaction of corrosion. These may also lead to high corrosion potential and low corrosion current.[39,40] Therefore, it can be concluded that both morphology and counter-anion would impact the anticorrosion effect of doped PANI.

## Conclusions

PANI nanofibers were prepared in four kinds of inorganic acids by direct mixed oxidation method. Especially in H$_2$SO$_4$, the best morphology with uniform diameter and several microns length was observed. IR and UV spectra of all the products obtained in different acids were similar. The study found that curing time of epoxy resin was delayed, when added with PANI. EIS analysis indicated that the optimum dosage of PANI (around 0.6%) existed, which improves the protective effect of epoxy coating.

Morphology and counter-anion would impact on the anticorrosion effect of the doped PANI. The results of this study showed that H$_3$PO$_4$-doped PANI showed the best protective effect, followed by H$_2$SO$_4$-doped PANI, and then followed by HNO$_3$-doped PANI. HCl-doped PANI provided the worst protective effect.

## References

1. Meroufel, A, Deslouis, C, Touzain, S, "Electrochemical and Anticorrosion Performances of Zinc-Rich and Polyaniline Powder Coatings." *Electrochim. Acta*, **53** (5) 2331–2338 (2008)
2. Yao, B, Wang, GC, Ye, JK, "Corrosion Inhibition of Carbon Steel by Polyaniline Nanofibers." *Mater. Lett.*, **62** (12) 1775–1778 (2008)
3. Lahav, M, Durkan, C, Willner, I, "Redox Activation of a Polyaniline-Coated Cantilever: an Electro-Driven Microdevice." *Angew. Chem.*, **113** (21) 4219–4221 (2001)
4. Alam, J, Riaz, U, Ahmad, S, "Development of Nanostructured Polyaniline Dispersed Smart Anticorrosive Composite Coatings." *Polym. Adv. Technol.*, **19** (7) 882–888 (2008)
5. Marcel, C, Tarascon, JM, "An All-Plastic WO$_3$.H$_2$O/Polyaniline Electrochromic Device." *Solid State Ionics*, **143** (1) 89–101 (2001)
6. Lu, JX, Moon, KS, Wong, CP, "High Dielectric Constant Polyaniline/Epoxy Composites via In Situ Polymerization for Embedded Capacitor Applications." *Polymer*, **48** (6) 1510–1516 (2007)
7. Deberry, DW, "Modification of the Electrochemical and Corrosion Behavior of Stainless Steel with Electroactive Coating." *J. Electrochem. Soc.*, **132** (5) 1022–1026 (1985)
8. Kraljic, M, Mandic, Z, Duic, LJ, "Inhibition of Steel Corrosion by Polyaniline Coatings." *Corr. Sci.*, **45** (1) 181–198 (2003)
9. Fang, JJ, Xu, K, Zhu, LH, "A Study on Mechanism of Corrosion Protection of Polyaniline Coating and Its Failure." *Corr. Sci.*, **49** (11) 4232–4242 (2007)
10. Williams, G, McMurray, HN, "Factors Affecting Acid-Base Stability of the Interface Between Polyaniline Emeraldine Salt and Oxide Covered Metal." *Electrochem. Solid-State Lett.*, **8** B42 (2005)
11. Rohwerder, M, Michalik, A, "Conducting Polymers for Corrosion Protection: What Makes the Difference between Failure and Success?" *Electrochim. Acta*, **53** (3) 1300–1313 (2007)
12. Rohwerder, M, Ducb, LM, Michalika, A, "In situ Investigation of Corrosion Localised at the Buried Interface Between Metaland Conducting Polymer Based Composite Coatings." *Electrochim. Acta*, **54** (25) 6075–6081 (2009)
13. Jing, XB, Wang, LX, Wang, XH, "Synthesis, Structure, Properties and Application of Conducting Polyaniline." *Acta Polym. Sin.*, **49** (5) 655–663 (2005)
14. Wessling, B, Posdorfer, J, "Corrosion Prevention with an Organic Metal (Polyaniline): Corrosion Test Results." *Electrochim. Acta*, **44** (12) 2139–2147 (1999)
15. Kalendova, A, Vesely, D, Stejskal, J, "Organic Coatings Containing Polyaniline and Inorganic Pigments as Corrosion Inhibitors." *Prog. Org. Coat.*, **62** (1) 105–116 (2008)
16. Akbarinezhad, E, Ebrahimi, M, Faridi, HR, "Corrosion Inhibition of Steel in Sodium Chloride Solution by Undoped Polyaniline Epoxy Blend Coating." *Prog. Org. Coat.*, **64** (4) 361–364 (2009)

17. Rout, TK, Jha, G, Singh, AK, "Development of Conducting Polyaniline Coating: a Novel Approach to Superior Corrosion Resistance." *Surf. Coat. Technol.*, **167** (1) 16–24 (2003)

18. Sathiyanarayanan, S, Azim, SS, "Performance Studies of Phosphate-Doped Polyaniline Containing Paint Coating for Corrosion Protection of Aluminium Alloy." *J. Appl. Polym. Sci.*, **107** (4) 2224–2230 (2008)

19. Chang, KC, Jang, GW, Peng, CW, "Comparatively Electrochemical Studies at Different Operational Temperatures for the Effect of Nanoclay Platelets on the Anticorrosion Efficiency of DBSA-doped Polyaniline/Na$^+$-MMT Clay Nanocomposite Coatings." *Electrochim. Acta*, **52** (16) 5191–5200 (2007)

20. Prakash, S, Rao, CRK, Vijayan, M, "New Polyaniline-Polyelectrolyte Composites: Synthesis and Applications." *Electrochim. Acta*, **53** (18) 5704–5710 (2008)

21. Ozyılmaz, AT, "The Corrosion Behavior of Polyaniline Top Coat on Nickel Plated Copper from Neutral Aqueous Medium." *Prog. Org. Coat.*, **54** 127–133 (2005)

22. Hur, E, Bereket, G, Sahin, Y, "Corrosion Inhibition of Stainless Steel by Polyaniline, Poly(2-chloroaniline), and Poly(aniline-*co*-2-chloroaniline) in HCl." *Prog. Org. Coat.*, **57** (2) 149–158 (2006)

23. Li, D, Huang, JX, Richard, BK, "Polyaniline Nanofibers: a Unique Polymer Nanostructure for Versatile Applications." *Acc. Chem. Res.*, **42** (1) 135–145 (2009)

24. Zhou, CQ, Han, J, Guo, R, "Synthesis of Polyaniline Hierarchical Structures in a Dilute SDS/HCl Solution: Nanostructure-Covered Rectangular Tubes." *Macromolecules*, **42** (4) 1252–1257 (2009)

25. Zhang, ZM, Wei, ZX, Wan, MX, "Nanostructures of Polyaniline Doped with Inorganic Acids." *Macromolecule*, **35** (15) 5937–5942 (2002)

26. Wu, CG, Bein, T, "Conducting Polyaniline Filaments in a Mesoporous Channel Host." *Science*, **264** (5166) 1757–1759 (1994)

27. Guo, YP, Zhou, Y, "Polyaniline Nanofibers Fabricated by Electrochemical Polymerization: A Mechanistic Study." *Eur. Polym. J.*, **43** (6) 2292–2297 (2007)

28. Dallas, P, Stamopoulos, D, Boukos, N, "Characterization, Magnetic and Transport Properties of Polyaniline Synthesized Through Interfacial Polymerization." *Polymer*, **48** (11) 3162–3169 (2007)

29. Huang, JX, Kaner, RB, "Nanofiber Formation in the Chemical Polymerization of Aniline: A Mechanistic Study." *Angew. Chem.*, **116** (43) 5941–5945 (2004)

30. Wei, ZX, Zhang, ZM, Wan, MX, "Formation Mechanism of Self-Assembled Polyaniline Micro/Nanotubes." *Langmuir*, **18** (3) 917–921 (2002)

31. Abdiryim, T, Zhang, XG, "Solid-State Reaction Synthesis and Characterization of Polyaniline Nanofibers Doped with Naphthalenesulfonic Acid." *Acta Polym. Sin.*, **47** (6) 858–861 (2003)

32. Wang, Y, Liu, ZM, Han, BX, "Facile Synthesis of Polyaniline Nanofibers Using Chloroaurate Acid as the Oxidant." *Langmuir*, **21** (3) 833–836 (2005)

33. Wang, T, Tan, YJ, "Understanding Electrodeposition of Polyaniline Coatings for Corrosion Prevention Applications Using the Wire Beam Electrode Method." *Corr. Sci.*, **48** (8) 2274–2290 (2006)

34. Cao, CN, *Principle of Electrochemical in Corrosion*. Chemical Industry Press, Beijing, 2004

35. Wang, YL, Jiang, ZH, Yao, ZP, "Microstructure and Corrosion Resistance of Ceramic Coating on Carbon Steel Prepared by Plasma Electrolytic Oxidation." *Surf. Coat. Technol.*, **204** (11) 1685–1688 (2010)

36. Huang, WS, MacDiarmid, AG, "Polyaniline, a Novel Conducting polymer." *J. Chem. Soc. Chem. Commun.*, **82** (1) 2385–2396 (1986)

37. Samui, AB, Patankar, AS, Rangarajan, J, "Study of Polyaniline Containing Paint for Corrosion Prevention." *Prog. Org. Coat.*, **47** (1) 1–7 (2003)

38. Kinlen, PJ, Menon, V, Ding, YW, "A Mechanistic Investigation of Polyaniline Corrosion Protection Using the Scanning Reference Electrode Technique." *J. Electrochem. Soc.*, **146** (10) 3690–3695 (1999)

39. Santos, JR, Mattoso, LHC, "Investigation of Corrosion Protection of Steel by Polyaniline Films." *Electrochem. Acta*, **43** (34) 309–313 (1998)

40. Ansari, R, Alikhani, AH, "Application of Polyaniline/Nylon Composites Coating for Corrosion Protection of Steel." *J. Coat. Technol. Res.*, **6** (2) 221–227 (2009)